ÉCOLE POLYTECHNIQUE
PROMOTION X 2022
Parcours d'Approfondissement : Energies
MOTA Victor

RESEARCH INTERNSHIP REPORT

MODELING AND SIMULATION OF LITHIUM PLATING IN BATTERIES WITH BATTMO

Non confidential report

Physics Department
Teacher advisor : Pere Roca

Internship tutor : Xavier Raynaud
Dates : 31/03/25 - 23/07/25

SINTEF
Forskningsveien 1
0373 Oslo, NORWAY

Déclaration d'intégrité relative au plagiat

Je soussigné(e) **M. Victor Mota** certifie sur l'honneur :

1. Que les résultats décrits dans ce rapport sont l'aboutissement de mon travail.
2. Que je suis l'auteur de ce rapport.
3. Que je n'ai pas utilisé des sources ou résultats tiers sans clairement les citer et les référencer selon les règles bibliographiques préconisées.

Mention à recopier :

> *Je déclare que ce travail ne peut être suspecté de plagiat.*

Date : .....

Signature : .....

Abstract

Le dépôt de lithium métallique (lithium plating) est un mécanisme majeur de dégradation dans les batteries lithium-ion, en particulier lors de charges rapides ou à basse température. Il entraîne non seulement une perte de capacité, mais présente aussi des risques importants pour la sécurité puisqu'il peut conduire à la formation de dendrites métalliques pouvant provoquer des courts-circuits internes et potentiellement conduire à une fuite thermique voire à l'explosion de la batterie.

Dans ce travail, nous avons implémenté un modèle physique de dépôt et de dissolution du lithium métallique dans le simulateur open-source *BattMo*, développé par SINTEF. L'implémentation comprend l'ajout de réactions interfaciales supplémentaires, une équation de conservation pour le lithium déposé, ainsi que des modifications aux équations d'équilibre de masse et de charge afin de prendre en compte la dynamique de couverture de surface de l'electrode.

Le modèle reproduit les principaux comportements décrits dans la littérature, notamment l'apparition du plating au delà d'un certain seuil de charge, le blocage de l'intercalation, la compétition entre les deux processus, et des pics transitoires d'intercalation lors du stripping. Bien que les simulations réalisées ici concernent une particule représentative unique, le modèle a été conçu de manière modulaire et peut facilement être étendu à des électrodes ou des cellules complètes. Ce travail pose ainsi les bases nécessaires à des développements futurs, notamment la modélisation du plating irréversible, de la croissance de dendrites en géométrie 3D, ou l'ajustement des paramètres pour des prédictions plus fiables en termes de performance et de sécurité.

Lithium plating is a critical degradation mechanism in lithium-ion batteries, especially under fast charging or low-temperature conditions. It not only leads to capacity loss but also poses serious safety risks through the formation of metallic dendrites, which can pierce the separator and trigger internal short circuits — potentially resulting in thermal runaway or even battery explosions.

In this work, we implemented a physically-based lithium plating and stripping model within the open-source *BattMo* simulation framework. The implementation includes additional interfacial reactions, a conservation equation for plated lithium, and modifications to the existing charge and mass balance equations to account for the electrode's surface coverage dynamics.

The model reproduces key behaviors observed in the literature, including plating onset, surface blocking, competition between intercalation and plating, and transient intercalation peaks during stripping. While the simulations presented here focus on a single representative particle, the model is designed to be modular and can be extended easily to simulate full battery cells or electrode assemblies. This foundational work enables future developments such as irreversible plating modeling, dendrite growth in realistic 3D geometries, and parameter calibration for predictive battery performance and safety analysis.

Contents

Acknowledgements

I would like to express my sincere gratitude to Xavier Raynaud, my internship supervisor, for his guidance during the four months of my internship. His kind and thoughtful advice enabled me to approach my tasks in the best possible conditions, both in terms of scientific knowledge and research methodology. The lessons I learned from him clearly went beyond the field of batteries and will stay with me for a long time to come.

I would also like to thank Halvor Nilsen for listening to me during the crucial moments of my internship, as well as Knut-Andreas Lie for welcoming me into his team.

I am deeply grateful to EDF's Sustainable Energy Chair for its financial support, which enabled me to complete my internship under the best conditions.

Last but not least, my sincere thanks go to all the SINTEF Digital Group for their warm welcome and constant kindness, as well as for their help with my Norwegian integration.

1 Introduction

Lithium-ion batteries are now ubiquitous in portable electronics, electric vehicles, and energy storage systems due to their high energy density and long cycle life. However, their performance and safety remain sensitive to operating conditions, particularly during fast charging. One of the most critical degradation mechanisms under such conditions is **lithium plating** — the deposition of metallic lithium on the negative electrode surface instead of insertion into the host material (typically graphite).

Lithium plating can lead to several problems. Initially, it reduces the amount of lithium available for intercalation, causing a loss of reversible capacity. More severely, the growth of metallic lithium can form filament-like structures known as **dendrites**. These dendrites may penetrate the separator and cause internal short circuits, which in turn can lead to thermal runaway and battery fires. Understanding and predicting the onset and evolution of lithium plating is therefore essential for improving battery safety and extending its lifetime.

Despite its importance, lithium plating remains difficult to model accurately due to its strongly nonlinear behavior and its dependence on spatial inhomogeneities. Most classical battery models neglect this phenomenon or treat it in a highly simplified way. The goal of this work is to incorporate a first physically-based lithium plating model into *BattMo*, an open-source MATLAB simulation framework developped by SINTEF. This addition lays the groundwork for simulating both reversible plating and stripping processes, and ultimately for capturing more complex degradation mechanisms such as dendrite formation or irreversible lithium loss.

The following sections present the theoretical basis of the model, the modifications made to the *BattMo* codebase, and the numerical results obtained under various operating scenarios.

2 Literature overview

The first step in this work was to get familiar with the various mechanisms and indicators of lithium plating in lithium-ion batteries, particularly during fast charging or low-temperature operation. Lithium plating is a critical issue as it can lead to capacity loss, internal short circuits, and thermal runaway. Numerous studies address lithium plating using different strategies, which can be roughly categorized into three approaches:

Electrochemical approach Lithium plating can often be inferred from electrochemical signatures, making these methods attractive due to their simplicity and compatibility with battery management systems. Coulombic efficiency (CE) analysis is widely used to detect lithium loss due to irreversible plating. High-precision CE measurements can reveal the onset of plating by identifying small but systematic deviations from ideal efficiency values [6]. Differential voltage analysis (DVA) and incremental capacity analysis (ICA) are also used to monitor subtle shifts in voltage profiles that indicate lithium deposition, especially during fast charging or low-temperature operation [13]. Electrochemical impedance spectroscopy (EIS) provides additional insight by detecting changes in the cell's impedance spectrum that correlate with lithium plating dynamics, particularly in the low-frequency region [7]. While these techniques are relatively easy to implement, they provide indirect evidence and can be difficult to disentangle from other degradation mechanisms. Some experimental protocols incorporate current rate or temperature variations to better isolate the effects of plating [2].

Post-mortem and in situ diagnostics More direct detection of lithium plating relies on advanced analytical and imaging techniques. In post-mortem studies, scanning electron microscopy (SEM) and X-ray photoelectron spectroscopy (XPS) are frequently used to directly confirm metallic lithium deposits on graphite anodes after cycling [10]. Quantification of "dead" lithium is also achievable via methods such as titration gas chromatography (TGC) and solid-state NMR [11]. Recently, ultrasound imaging has emerged as a promising *operando* technique. A study by Wasylowski *et al.* (2024) demonstrated a scanning acoustic microscopy (SAM) method capable of non-invasively visualizing plating and stripping in pouch cells with $\sim$75 μm spatial resolution [12]. These combined approaches enable quantification of inactive lithium while enabling dynamic observation—albeit at the expense of equipment complexity and cost.

Modeling approach Finally, many recent works propose modeling frameworks that describe the conditions under which lithium plating is likely to occur. Lithium plating is modeled as a chemical reaction competing with the lithium intercalation in the electrode [4]. Models vary in complexity, as lithium deposition can be modeled as reversible or partially reversible [8]. In addition, the complex geometry of the dendrites formed by plating is studied in some articles [9], although most publications study the quantity of lithium plated without taking into account its geometry.

The base reference used for this modeling work is [4].

3 Battmo presentation

3.1 Project objective and BattMo framework

The objective of this project was to extend the *BattMo* simulation platform by implementing a model for lithium plating and stripping. *BattMo* is an open-source, object-oriented battery modeling tool written in MATLAB, designed to simulate lithium-ion cells. It provides a modular architecture that allows researchers to couple various physical submodels — such as electrochemical kinetics, thermal behavior, or degradation mechanisms — within a unified and extensible environment.

Until now, *BattMo* focused on lithium-ion intercalation processes and did not account for metallic lithium deposition. The work presented here introduces the lithium plating phenomenon as an additional interfacial reaction, enabling the simulation of degradation modes occurring under high-rate charging or low-temperature conditions.

3.2 The P2D model framework

The P2D (Pseudo-Two-Dimensional) model, originally introduced in [3], is a widely used framework for simulating the electrochemical behavior of lithium-ion batteries. It captures both macroscopic and microscopic transport phenomena by coupling a one-dimensional description of the porous electrode and electrolyte domains with a radial model for lithium diffusion inside spherical active material particles.

In the P2D model, each electrode is represented along the macroscopic x-axis, which spans the thickness of the cell from current collector to separator. Within each position x, the electrode is composed of a representative spherical particle, inside which lithium diffusion is described along the radial coordinate r. The electrolyte phase is modeled as a continuous medium throughout the electrode and separator, allowing for ionic transport and potential gradients.

This multiscale structure enables the model to resolve key physical processes:

- Lithium-ion transport in the electrolyte,
- Electric potential distribution in both solid and electrolyte phases,
- Lithium intercalation dynamics within particles,
- Reaction kinetics at the electrode/electrolyte interface.

The P2D model provides a physically rich yet computationally tractable approximation of the full 3D porous electrode geometry. It serves as the foundation for most high-fidelity battery modeling tools, as the P4D model and can be extended to incorporate additional physics such as lithium plating, SEI formation, thermal effects, or mechanical deformation.

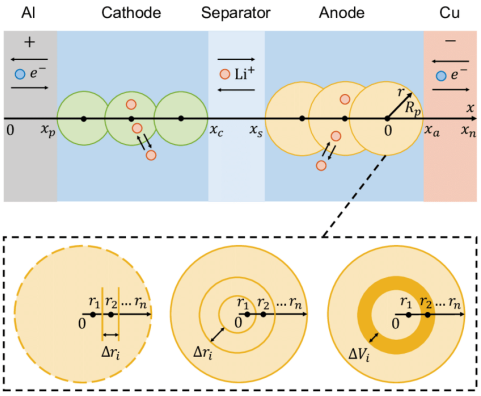

Figure 1: Schematic illustration of the P2D model, showing the spatial coordinate x across the macro-scale domain (top), and the radial discretization in the active material particles (bottom). Adapted from [5].

3.3 BattMo functionning

BattMo is a complex MATLAB software which has been developed by SINTEF for a few years and which is not trivial to understand at first glance because of the numerous possibilities of battery simulation that it offers. The model implements a great number of coupled equations, used to compute a dozen of primary variables. An accurate understanding of the physical processes as well as a rigorous lecture of the code was then necessary to fully grasp its functioning. The models implemented in *BattMo* are often composed of two porous electrodes separated by a separator avoiding short-circuits and possible dendrites growth. Each of the porous electrode is composed of active material spherical particles and of an electrolyte who completely fills the pores.

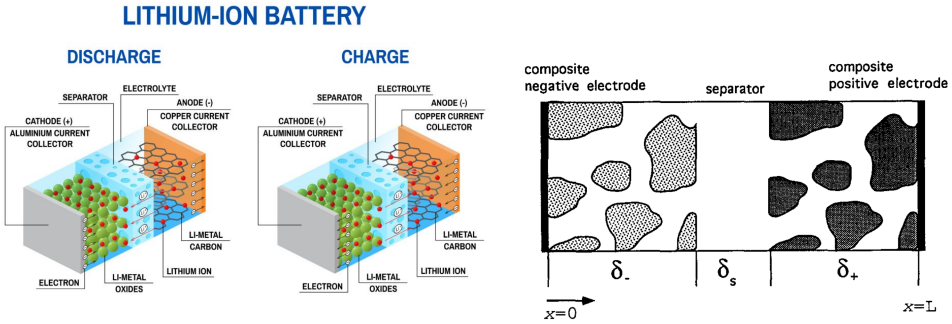

Figure 2: Illustration of a Li-ion battery battery with composite electrodes

Source: Dreamstime.com

The code is then organized with super-classes and subclasses which are for some only useful to set a proper environment and for some others at the heart of the simulation as they have a physical meaning. This classes with a physical sense have their own set of input parameters defined in a separate `json` file which can be read thanks to the associated `InputParams` classes. A simplified schema of the meaningful classes is given below.

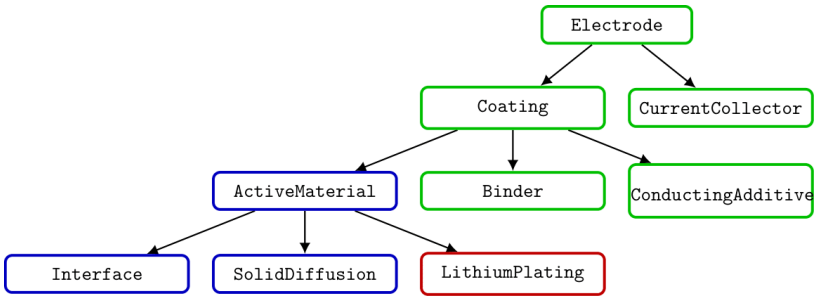

Figure 3: Simplified diagram of an electrode model using *BattMo*. Classes modified in the course of this work are shown in blue, while the newly introduced `LithiumPlating` class appears in red.

In this structure are implemented all different meaningful physical equations, depending on parameters and physical properties set by the users and on the unknown factors. To summarize, in the classical model, there are eleven primary variables (given below) and thus eleven fundamental equations to solve (these equations are given in Appendix A).

c_{elyte}	Lithium ion concentration in the electrolyte
ϕ_{elyte}	Potential of the electrolyte
c_{pe}	Lithium concentration in a positive electrode particle
c_{ne}	Lithium concentration in a negative electrode particle
ϕ_{pe}	Potential at the surface of the positive electrode particles
ϕ_{ne}	Potential at the surface of the negative electrode particles
$c_{pe,surface}$	Concentration at the surface of the positive electrode particles
$c_{ne,surface}$	Concentration at the surface of negative electrode particles
I	Global current of the battery
E	Global voltage of the battery
T	Temperature

Table 1: primary variables of the model

Appendix B presents the initial and boundary conditions for the study as well as the evolutions laws for some important parameters depending on the primary variables.

3.4 Dependency structure of the Lithium Plating sub-model

Figure 4 shows the computational dependency graph of the `LithiumPlating` sub-model implemented in *BattMo*. The graph illustrates how all internal variables of the model are derived from a **primary variable**: `platedConcentrationNorm`. This normalized concentration (unitless) is the only state variable in the model that is directly manipulated by the numerical solver.

Starting from this primary input, all other variables are computed in a specific order determined by the directed graph. The calculation propagates through the network until it reaches the variable `platedConcentrationCons`, located at the bottom of the graph. This variable represents the conservation equation of plated lithium and acts as a **residual function**: the solver iteratively adjusts `platedConcentrationNorm` so that `platedConcentrationCons` approaches zero. When this condition is satisfied (i.e., the residual is below a convergence threshold), the solver accepts the time step and moves forward in the simulation.

Several input nodes in the graph — such as `T`, `phiElectrode`, `phiElectrolyte`, `OCP`, and `cElectrolyte` — have no parents within the sub-model. These variables are computed in other *BattMo* models (e.g., ActiveMaterial, SolidDiffusion) but are required to evaluate the plating kinetics and thermodynamics.

One variable deserves special mention: `platedThickness`. Although it depends on `platedConcentration`, it has no children and does not appear in any conservation law. This variable plays no role in the numerical solution; it is marked as a passive "extra variable" in the model and is computed solely for visualization or post-processing purposes.

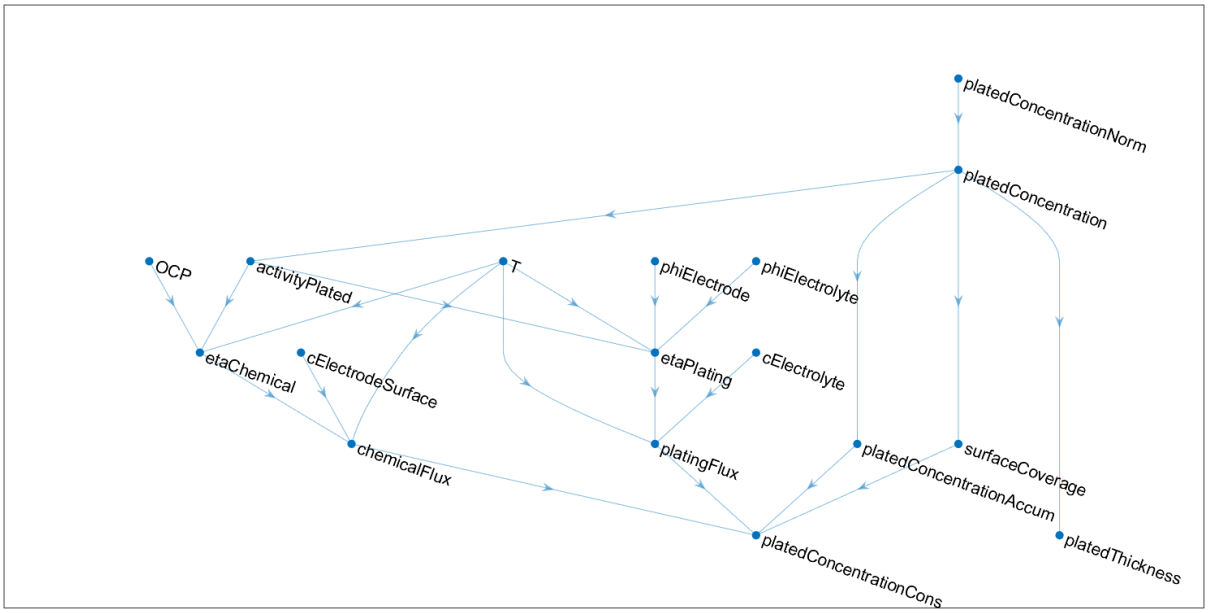

Figure 4: Dependency graph of the `LithiumPlating` sub-model. The solver adjusts the top node (`platedConcentrationNorm`) until the residual at the bottom node (`platedConcentrationCons`) is minimized.

Variable	Description
platedConcentrationNorm	Primary state variable (normalized concentration of plated lithium), controlled by the solver.
platedConcentration	Actual concentration of plated lithium [mol/m^3], scaled from the normalized variable.
activityPlated	Activity of plated lithium, used in the Butler–Volmer kinetics and regularized to avoid singularities.
etaPlating	Overpotential driving the plating/stripping reaction [V].
etaChemical	Overpotential for chemical intercalation of plated lithium into graphite [V].
platingFlux	Molar flux of lithium metal being plated or stripped [mol/m^2/s].
chemicalFlux	Molar flux of plated lithium chemically inserting into the active material [mol/m^2/s].
platedConcentrationAccum	Time derivative (accumulation) of plated lithium concentration [mol/m^3/s].
surfaceCoverage	Fraction of the surface covered by plated lithium ($\theta \in [0, 1]$).
platedConcentrationCons	Residual of the conservation equation for plated lithium; the solver seeks to minimize this value.
platedThickness	Equivalent thickness of the plated lithium layer [m]; used for visualization only.
OCP	Open-circuit potential of the graphite electrode [V].
T	Temperature of the system [K].
phiElectrode	Electric potential in the solid electrode phase [V].
phiElectrolyte	Electric potential in the electrolyte [V].
cElectrolyte	Lithium-ion concentration in the electrolyte [mol/m^3].
cElectrodeSurface	Lithium concentration at the surface of the active material particle [mol/m^3].

Table 2: Description of the variables used in the LithiumPlating sub-model.

4 Presentation of the selected model

Even if *BattMo* offers the possibility to simulate a wide range of battery phenomena, it does not natively include lithium plating mechanisms, which can occur during fast charging or at low temperatures. The objective of this work was to implement a consistent and physically motivated model of lithium plating and stripping at the negative electrode surface.

The original model developed by Hein, Danner and Latz [4] is formulated at the scale of a single representative particle. As such, the governing equations are expressed in terms of extensive quantities (e.g., total amount of lithium plated per particle in mol), which are well suited for detailed mechanistic analysis at the particle level.

In contrast, *BattMo* is designed to simulate battery electrodes composed of many particles and relies on **intensive** variables such as concentrations ($\mathrm{mol/m^3}$) and fluxes per unit volume ($\mathrm{mol/m^3/s}$). This formulation facilitates the assembly and coupling of representative particles within porous electrode models.

To integrate the plating model into *BattMo*'s framework, all extensive expressions from the original work were reformulated in intensive terms. For example, the plated lithium surface density ($\mathrm{mol/m^2}$) is converted to a volumetric concentration using the electrode's volumetric surface area, and all interfacial fluxes are scaled accordingly.

4.1 Intercalation, plating and chemical intercalation reactions

The selected model is based on the work of Hein, Danner and Latz [4], in which lithium plating is introduced as a **parallel reaction** to intercalation, governed by Butler–Volmer kinetics. In this framework, three electrochemical processes may occur at the negative electrode surface:

- **Intercalation** of lithium ions into graphite:

$$\mathrm{Li^+_{elyte}} + e^- \rightarrow \mathrm{Li_{graphite}}$$

- **Plating/Stripping** of lithium metal (electrochemical reduction and deposition at the surface):

$$\mathrm{Li^+_{elyte}} + e^- \rightarrow \mathrm{Li_{pl}}$$

- **Chemical intercalation** of previously deposited lithium (oxidation and dissolution):

$$\mathrm{Li_{pl}} \rightarrow \mathrm{Li_{graphite}}$$

All fluxes in this model are defined using the convention that they are positive when directed from the *interior* of the active material toward the *electrolyte* (i.e., outward flux from the particle surface). As a result:

- The **intercalation flux** is negative during lithiation ($\mathrm{Li^+}$ entering the particle), and positive during delithiation.

- The **plating flux** is negative when lithium metal is being deposited (plating), and positive when stripped.
- The **chemical intercalation flux** (insertion of plated lithium into the particle) is negative when lithium transfers from the metallic layer into the solid phase.

This model describes all processes as *reversible* and does not include irreversible mechanisms such as SEI growth, or dead lithium formation. The implemented framework therefore assumes that all deposited lithium can eventually be stripped or re-intercalated into the graphite.

4.2 Surface coverage and layered plating mechanism in the Hein model

In the model proposed by Hein, Danner and Latz [4], lithium plating is assumed to proceed in a layer-by-layer fashion. Each monolayer corresponds to a fixed surface density of lithium, beyond which additional lithium is deposited in subsequent layers. This behavior is captured by tracking the total amount of plated lithium and comparing it to the quantity required to cover the surface of a particle with a single atomic layer.

To integrate this into *BattMo*'s volumetric formulation, the surface-based monolayer quantity is converted into an equivalent concentration threshold c_{limit} [mol/m^3]. This threshold defines the plated lithium concentration required to form one full monolayer around a particle:

$$c_{\text{limit}} = \frac{n_{\text{pl}}^{\text{1ML}} \cdot \varepsilon}{\frac{4}{3}\pi r^3} \tag{1}$$

where:

- $n_{\text{pl}}^{\text{1ML}}$ is the surface density of lithium required to cover the particle with one monolayer [mol/m^2], computed as in [4] (See Appendix C for more details),
- ε is the volume fraction of active material,
- r is the particle radius.

The fraction of the particle surface covered by lithium is then expressed as:

$$\theta = \min\left(1, \frac{c_{\text{pl}}}{c_{\text{limit}}}\right) \tag{2}$$

This surface coverage factor $\theta \in [0, 1]$ is critical to the model, as it modulates the availability of the active surface for interfacial reactions. All volumetric fluxes (e.g., intercalation, plating, chemical intercalation) are multiplied by a surface factor, which ensures that:

- When $\theta << 1$, the surface is fully available for intercalation and plating. However, in this case, very little lithium plating can actually occur, because the plating

reaction is assumed to take place *on top of existing plated lithium*. Since the reaction site is effectively the lithium metal itself, a vanishing θ would prevent any further plating. In practice, this situation is avoided by initializing the plated lithium concentration to a small but nonzero value (see next subsection), so that some metallic lithium is always present and plating can proceed.

- When $\theta = 1$, the surface is fully covered by plated lithium and direct intercalation is suppressed.

This last point is particularly important: even if the intercalation flux N_{int} is nonzero according to its kinetic expression, it is effectively disabled in the conservation equations when $\theta = 1$, ensuring that lithium cannot intercalate through a surface blocked by metallic lithium.

4.3 Kinetics

4.3.1 Intercalation kinetics

The intercalation of lithium ions into graphite particles is modeled using a classical Butler–Volmer expression for the interfacial molar flux N_{int} [mol/m^2/s], describing the charge-transfer reaction at the electrolyte/electrode interface,

$$\text{Li}^+_{\text{elyte}} + e^- \rightleftharpoons \text{Li}_{\text{graphite}} \tag{3}$$

$$N_{\text{int}} = k_{\text{int}} \cdot \sqrt{c_{\text{elyte}}} \cdot \sqrt{c_{\text{surf}}} \cdot \sinh\left(\frac{F\eta_{\text{int}}}{RT}\right), \tag{4}$$

where the intercalation overpotential η_{int} is

$$\eta_{\text{int}} = \phi_{\text{el}} - \phi_{\text{elyte}} - U(c_{\text{surf}})$$

and

- k_{int} is the reaction rate constant for intercalation,
- c_{elyte} is the lithium ion concentration in the electrolyte,
- c_{surf} is the lithium concentration at the particle surface,
- F, R, and T are the Faraday constant, gas constant, and temperature, respectively.

4.3.2 Lithium plating and stripping kinetics

Lithium metal deposition (plating) and removal (stripping) at the negative electrode are described through a unified Butler–Volmer-type expression. The interfacial molar flux N_{pl} (in mol $\cdot$ m^{-2} $\cdot$ s^{-1}) is defined as:

$$N_{\text{pl}} = N_{0,\text{pl}} \left[\exp\left(\frac{\alpha F\eta_{\text{pl}}}{RT}\right) - \exp\left(-\frac{(1-\alpha)F\eta_{\text{pl}}}{RT}\right)\right], \tag{5}$$

where

- N_{pl} is the molar flux of lithium metal at the electrode/electrolyte interface,
- $N_{0,\text{pl}}$ is the exchange molar flux,
- η_{pl} is the plating/stripping overpotential,
- F is Faraday's constant,
- α is the charge transfer coefficient,
- R is the universal gas constant,
- T is the temperature.

The overpotential η_{pl} is given by

$$\eta_{\text{pl}} = \phi_{\text{el}} - \phi_{\text{elyte}} + \frac{RT}{F} \ln\left(a_{\text{pl}}\right) \tag{6}$$

where the activity a_{pl} of plated lithium accounts for the effect of surface coverage and is defined as

$$a_{\text{pl}} = \frac{c_{\text{pl}}^4}{c_{\text{pl}}^4 + c_{\text{pl},0}^4}. \tag{7}$$

Here, we have

- c_{pl} is the local volumetric concentration of plated lithium ($\text{mol} \cdot \text{m}^{-3}$),
- $c_{\text{pl},0}$ is a regularization parameter used to prevent singularities at low concentrations (e.g., $c_{\text{pl},0} = 10^{-6} \cdot c_{\text{limit}}$) computed from the phenomenological parameter $n_{\text{pl},0}$ introduced in [4], the particle radius, and the volume fraction:

$$c_0 = \frac{n_{\text{pl},0} \cdot \varepsilon}{\frac{4}{3}\pi r^3}$$

The exchange molar flux is defined as

$$N_{0,\text{pl}} = k_{\text{pl}} \left(c_{\text{elyte}}\right)^{\alpha}, \tag{8}$$

assuming a constant activity for metallic lithium (i.e., $c_{\text{Li}^0} = 1$).

The plating reaction is in direct **competition** with the intercalation reaction, as both draw lithium ions and electrons from the same interfacial region. The plating process may become thermodynamically and kinetically favored under certain conditions — particularly at low surface potentials (i.e., strongly negative overpotentials) or high applied currents.

In such regimes, a significant portion of the total current can be diverted into metallic lithium deposition instead of intercalation, especially when the active material approaches full lithiation (i.e., the electrode potential becomes close to that of Li/Li^+). The interplay between the two reactions is modulated by their respective kinetics but also by surface accessibility, which is regulated through the surface coverage factor θ.

4.3.3 Chemical intercalation kinetics and lithium insertion through plated layers

In addition to direct electrochemical intercalation from the electrolyte, the model incorporates a secondary mechanism: **chemical intercalation** of lithium from the metallic plated layer into the graphite electrode. This reaction allows plated lithium atoms to diffuse into the solid active material without the involvement of the electrolyte or external current. It is modeled as a Butler–Volmer-type process:

$$\mathrm{Li}^0_{\mathrm{pl}} \rightleftharpoons \mathrm{Li}_{\mathrm{graphite}} \tag{9}$$

$$N_{\mathrm{chem}} = k_{\mathrm{chem}} \cdot \sqrt{c_{\mathrm{surf}}} \cdot \sinh\left(\frac{F\eta_{\mathrm{chem}}}{RT}\right) \tag{10}$$

where the chemical intercolation overpotential is

$$\eta_{\mathrm{chem}} = -U(c_{\mathrm{surf}}) - \frac{RT}{F}\ln(a_{\mathrm{pl}}) \tag{11}$$

and

- k_{chem} is the rate constant for chemical intercalation,
- c_{surf} is the lithium concentration at the surface of the particle

This reaction plays a critical role in certain operating conditions — particularly when the surface coverage θ reaches unity, i.e., when the graphite surface is fully covered by a metallic lithium layer. In this state, direct intercalation from the electrolyte is blocked due to the absence of available surface. However, the *chemical intercalation* flux remains active because it occurs within the plated layer itself and does not require direct access to the graphite surface from the electrolyte side.

As a result, the electrode can **continue to fill marginally even when** $\theta = 1$, provided that the chemical overpotential drives the insertion — a feature that reflects experimental observations hence [4]

The overpotentials η_{int}, η_{pl} and η_{chem} are not independent. We can check from their expression that they satisfy the following relationship

$$\eta_{\mathrm{int}} = \eta_{\mathrm{pl}} + \eta_{\mathrm{chem}}. \tag{12}$$

4.4 Modifications and additions to conservation equations

The inclusion of lithium plating in the model requires the introduction of a new state variable, the concentration of plated lithium c_{pl}, and the corresponding modifications to existing conservation equations. Four main changes were made:

1. Surface coverage scaling. All new flux terms are scaled by the surface coverage factor $\theta \in [0, 1]$, which is computed as the ratio of the current plated lithium amount to the amount required for full monolayer coverage. This ensures that:

- The plating flux is only active where some coated surface area is available.
- The intercalation and chemical fluxes are suppressed when the surface is fully covered with metallic lithium.

These changes collectively ensure mass and charge consistency in the presence of dynamically evolving lithium metal deposits at the electrode surface.

2. Addition of a conservation equation for plated lithium. A new conservation equation was introduced to track the time evolution of the plated lithium concentration. The plated lithium is stored as a surface quantity ($\mathrm{mol/m^2}$) but is expressed in terms of a volumetric concentration ($\mathrm{mol/m^3}$) using the volumetric surface area of the electrode. The equation reads

$$\frac{\partial c_{\mathrm{pl}}}{\partial t} = a_{\mathrm{v}} \theta \left(N_{\mathrm{chem}} - N_{\mathrm{pl}} \right), \tag{13}$$

where

- θ is the surface coverage factor (between 0 and 1), accounting for the fraction of surface available for the reactions,
- a_{v} is the volumetric surface area [$\mathrm{m^2/m^3}$],
- N_{pl} is the plating/stripping molar flux [$\mathrm{mol/m^2/s}$],
- N_{chem} is the flux of chemical intercalation of plated lithium into the electrode.

3. Modification of the charge conservation equation. The total interfacial current now includes contributions from both the intercalation and the plating reactions. The current density at the particle surface becomes

$$i_{\mathrm{interface}} = F \cdot a_{\mathrm{v}} \left((1 - \theta) N_{\mathrm{int}} + \theta N_{\mathrm{pl}} \right), \tag{14}$$

where N_{int} is the intercalation flux and F is Faraday's constant. The flux N_{pl} and N_{int} are signed, and counted positive from the inside of the particle to the electrolyte. In particular, N_{pl} is negative during plating.

4. Modification of the lithium mass balance in the solid phase. The rate of change of lithium concentration within the active material must now include the contribution from the chemical intercalation of plated lithium:

$$\frac{\partial c_{\mathrm{graphite}}}{\partial t} = a_{\mathrm{v}} \cdot \left(- (1 - \theta) N_{\mathrm{int}} - \theta N_{\mathrm{chem}} \right) \tag{15}$$

where the flux N_{chem} accounts for the transfer of lithium from the plated metallic layer into the solid electrode structure.

4.5 Initial condition for plated lithium concentration

We choose to initialize the quantity of plated lithium so that the simulation starts at equilibrium. At equilibrium, the time derivatives of all governing equations vanish. In particular, the conservation equation for lithium in the electrolyte is given by

$$\frac{\partial c_{\text{elyte}}}{\partial t} = a_v(-\theta N_{\text{pl}} - (1-\theta)N_{\text{int}}), \tag{16}$$

and must be zero at $t = 0$, along with the conservation laws for plated lithium (13) and lithium in the solid phase (15). This leads to the algebraic equilibrium conditions

$$\theta(N_{\text{chem}} - N_{\text{pl}}) = 0, \tag{17}$$
$$(1-\theta)N_{\text{int}} + \theta N_{\text{chem}} = 0, \tag{18}$$
$$-\theta N_{\text{pl}} - (1-\theta)N_{\text{int}} = 0. \tag{19}$$

If the surface coverage θ is zero, then equations (17) to (19) reduce to $N_{\text{int}} = 0$, while plating is disabled due to the absence of metallic lithium. To avoid this degenerate situation, we initialize the system with a small but positive $\theta > 0$. In particular, we assume that $\theta < 1$.

For any $\theta \in (0, 1)$, the only possible solution to the system is

$$N_{\text{int}} = N_{\text{pl}} = N_{\text{chem}} = 0,$$

which is equivalent to requiring that the associated overpotentials vanish

$$\eta_{\text{int}} = \eta_{\text{pl}} = \eta_{\text{chem}} = 0.$$

We now determine the variables consistent with this equilibrium. The intercalated lithium concentration c_{graphite}, or equivalently the open-circuit potential $U(c_{\text{surf}})$, is assumed known. The electrolyte potential is set to zero by convention, $\phi_{\text{elyte}} = 0$. This leaves two unknowns: the solid potential ϕ_{el} and the plated lithium concentration c_{pl}.

At first glance, the three conditions $\eta_{\text{int}} = \eta_{\text{pl}} = \eta_{\text{chem}} = 0$ appear to overconstrain the system. However, these overpotentials are not independent: equation (12) shows that they are related. In practice, we only need to enforce two of them. We decide to use

$$\eta_{\text{int}} = \phi_{\text{el}} - \phi_{\text{elyte}} - U(c_{\text{surf}}) \tag{20}$$
$$\eta_{\text{chem}} = -U(c_{\text{surf}}) - \frac{RT}{F}\ln(a_{\text{pl}}) \tag{21}$$

The first condition gives the initial electrode potential

$$\phi_{\text{el}} = U(c_{\text{surf}}), \tag{22}$$

while the second yields the required activity of plated lithium

$$a_{\text{pl}} = \exp\left(-\frac{FU(c_{\text{surf}})}{RT}\right), \tag{23}$$

where the activity a_{pl} of plated lithium accounts for the effect of surface coverage and is defined as

$$a_{\mathrm{pl}} = \frac{c_{\mathrm{pl}}^4}{c_{\mathrm{pl}}^4 + c_{\mathrm{pl},0}^4}. \tag{24}$$

Here, we have

- c_{pl} is the local volumetric concentration of plated lithium ($\mathrm{mol} \cdot \mathrm{m}^{-3}$),
- $c_{\mathrm{pl},0}$ is a regularization parameter used to prevent singularities at low concentrations (e.g., $c_{\mathrm{pl},0} = 10^{-6} \cdot c_{\mathrm{limit}}$), computed from the phenomenological parameter $n_{\mathrm{pl},0}$ introduced in [4], the particle radius r, and the volume fraction ε, using the expression

$$c_{\mathrm{pl},0} = \frac{n_{\mathrm{pl},0} \cdot \varepsilon}{\frac{4}{3}\pi r^3}.$$

By combining both expressions for a_{pl}, we obtain the initial concentration of plated lithium, which is

$$c_{\mathrm{pl}} = c_{\mathrm{pl},0} \cdot \left(\exp\left(-\frac{FU(c_{\mathrm{surf}})}{RT} \right) - 1 \right)^{1/4}. \tag{25}$$

This ensures that all fluxes and overpotentials vanish at $t = 0$, so the system starts in a fully consistent electrochemical equilibrium, which means

$$\eta_{\mathrm{int}} = \eta_{\mathrm{pl}} = \eta_{\mathrm{chem}} = 0 \qquad \text{and} \qquad N_{\mathrm{int}} = N_{\mathrm{pl}} = N_{\mathrm{chem}} = 0.$$

5 Results

The implemented model successfully reproduces lithium plating and stripping behavior, in qualitative agreement with the results reported in [4]. Under lithium saturation near the particle surface, we observe the onset of metallic lithium deposition, followed by stripping or reinsertion depending on the cycling conditions. While some quantitative differences remain due to parameter choices and model reformulations, the core mechanisms and trends are preserved.

In the following subsections, we investigate how key physical parameters influence the plating dynamics. We focus in particular on the competition between intercalation and plating currents and we take the example of temperature to show how a physical parameter can significantly alter the importance of the plating phenomenon.

5.1 Observation of lithium plating and characteristic phases

Our simulations confirm that lithium plating is correctly triggered under suitable conditions. Figure 5 shows the evolution of the surface lithium concentration (blue curve) and the volumetric plating flux (orange curve) over time, for a charge-discharge scenario. The charge and discharge currents have the same constant value and the switch is voltage controlled. The system exhibits the expected sequence of plating and stripping phenomena, with distinct physical phases:

1. **Charging without plating (0–5 s):** At the beginning of the simulation, the surface concentration increases steadily as lithium intercalates into the electrode. The plating flux remains essentially zero during this period, indicating that all the lithium is entering the particle through intercalation.

2. **Onset of plating (5-12 s):** Once the surface concentration approaches $\sim$ 30 mol/L — near the maximum solid concentration of the electrode — the plating flux begins to rise sharply. This threshold corresponds to the condition where intercalation slows due to surface saturation, and so the plating reaction becomes favorable. As plating proceeds, more of the particle surface becomes covered with metallic lithium, increasing the effective area for the plating reaction. This leads to a positive feedback loop where the plating flux grows rapidly with time.

3. **Electrode saturation and flux stabilization (12-22 s):** As the surface becomes fully covered with plated lithium ($\theta = 1$), the active reaction area of the plating reaction reaches its maximum. Moreover, no further direct intercalation can occur. The electrode potential, previously evolving due to the intercalation reaction, stabilizes once intercalation stops, which in turn fixes the overpotential and thus the reaction rate of plating. This explains the flat section of the plating flux curve.

4. **Stripping phase at start of discharge (22-32 s):** When the direction of current reverses, the system enters the stripping regime. The flux becomes positive, indicating oxidation and dissolution of lithium metal back into the electrolyte. Initially, the flux is high due to the fully plated surface.

5. **Surface reopening and intercalation recovery (32–45 s):** As stripping removes part of the plated layer, the surface becomes partially uncovered ($\theta < 1$). This reduces the active area for stripping, leading to a gradual decrease in the stripping flux. Simultaneously, intercalation can resume where surface becomes available, allowing surface concentration to decrease further.

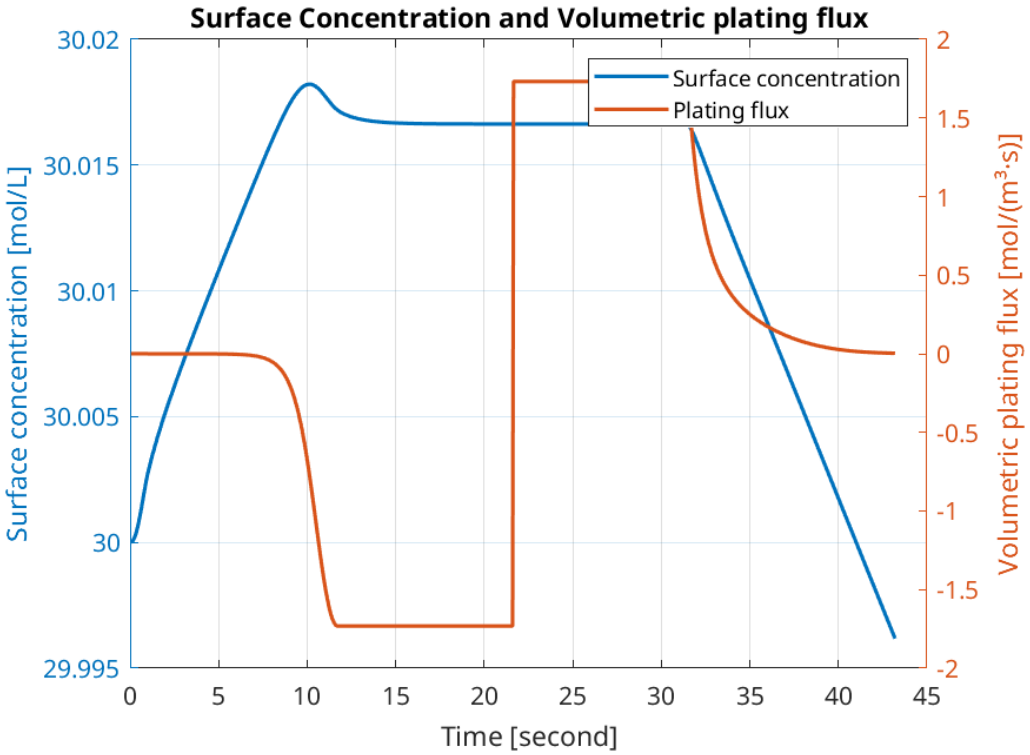

Figure 5: Surface lithium concentration (blue) and volumetric plating flux (orange) as functions of time. The plot illustrates the sequence of plating onset, surface saturation, flux stabilization, and subsequent stripping.

5.2 Complementarity of plating and intercalation currents

Figure 6 illustrates the normalized intercalation and plating currents as a function of time, expressed as percentages of the applied current $I_{\max}$, under two different kinetic regimes.

The kinetic constants used in the original model by Hein et al. were unusually high — typically on the order of 10^3 — whereas values reported in the broader battery modeling literature are often around 10^{-9} m/s (e.g., Arora et al., 1999 [1]). These large values led to strong numerical stiffness and convergence issues in our simulations. To address this, we replaced the original constants k_{pl}, k_{int}, and k_{chem} with more realistic values drawn from Arora's work, as detailed in Appendix C. To highlight the plating effect, we increased k_{pl}.

In Figure 6a, we use strongly asymmetric kinetics with $k_{\text{pl}} \approx 10^3 \cdot k_{\text{int}}$, resulting in well-separated regimes dominated either by plating or intercalation. Each current switches sharply as the electrode transitions between lithiation and delithiation. The two processes are strictly complementary, their sum always matching the applied current.

In contrast, Figure 6b shows results for a milder asymmetry, $k_{\text{pl}} \approx 10^2 \cdot k_{\text{int}}$, which is closer to the original configuration used by Hein et al. In this case, plating and intercalation occur with more similar kinetics, leading to the emergence of a transient **intercalation current peak** during the onset of stripping.

This peak arises when the plated lithium layer begins to dissolve, uncovering previously blocked graphite regions. Intercalation briefly reactivates before the system re-establishes equilibrium between stripping and insertion.

This behavior is characteristic of the **local current loop** mechanism described by Hein et al in [4]. During this phase, stripping and intercalation occur simultaneously but in opposite directions: lithium is oxidized at the metallic surface (stripping) and reinserted into graphite via intercalation. Since the same interface mediates both processes, a portion of the current loops internally through the electrode, bypassing the external circuit. This loop accelerates stripping, as not all lithium returns to the electrolyte—some is immediately reintegrated into the host material.

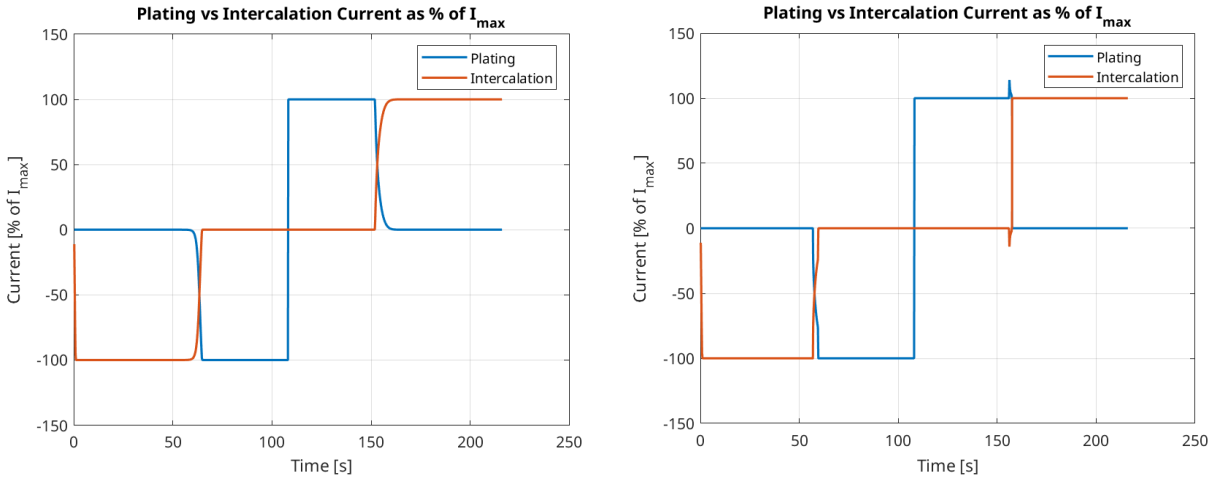

(a) Arora et al. parameters ($k_{\text{pl}} \approx 10^3 \cdot k_{\text{int}}$). (b) Reduced asymmetry ($k_{\text{pl}} \approx 10^2 \cdot k_{\text{int}}$).

Figure 6: Normalized intercalation and plating currents (as % of I_{max}) under two kinetic regimes.

5.3 Influence of temperature on lithium plating dynamics

Temperature plays a critical role in the dynamics of lithium plating in lithium-ion batteries. This influence stems primarily from its effect on lithium diffusion within the solid active material. At lower temperatures, lithium ions diffuse more slowly into the interior of the particle. As a result, lithium tends to accumulate near the surface more quickly, raising the surface concentration and accelerating the onset of lithium plating.

Figure 7 shows the evolution of the surface lithium concentration (solid lines) and the surface coverage θ (dashed lines) over time at three different temperatures (150 K, 250 K, and 350 K). At low temperature (blue curves, 150 K), the surface concentration increases rapidly and reaches a critical value earlier than at higher temperatures. This early saturation of the surface triggers substantial lithium plating.

Once the plating process is activated and the surface becomes progressively covered by

metallic lithium, direct intercalation is suppressed. However, lithium that was accumulated at the surface continues to diffuse inward into the particle bulk. This causes the surface concentration to decrease after reaching its maximum, as observed in all three cases — more markedly at lower temperatures where the diffusion lag is greater.

Furthermore, the final state of charge of the particle is also temperature-dependent. At low temperatures, the slower diffusion prevents the complete lithiation of the particle interior. As a result, the total amount of lithium stored in the particle is reduced, leading to a lower overall state of charge at the end of the simulation. This is visible in Figure 7 through the lower final surface concentration and the persistent surface coverage plateau.

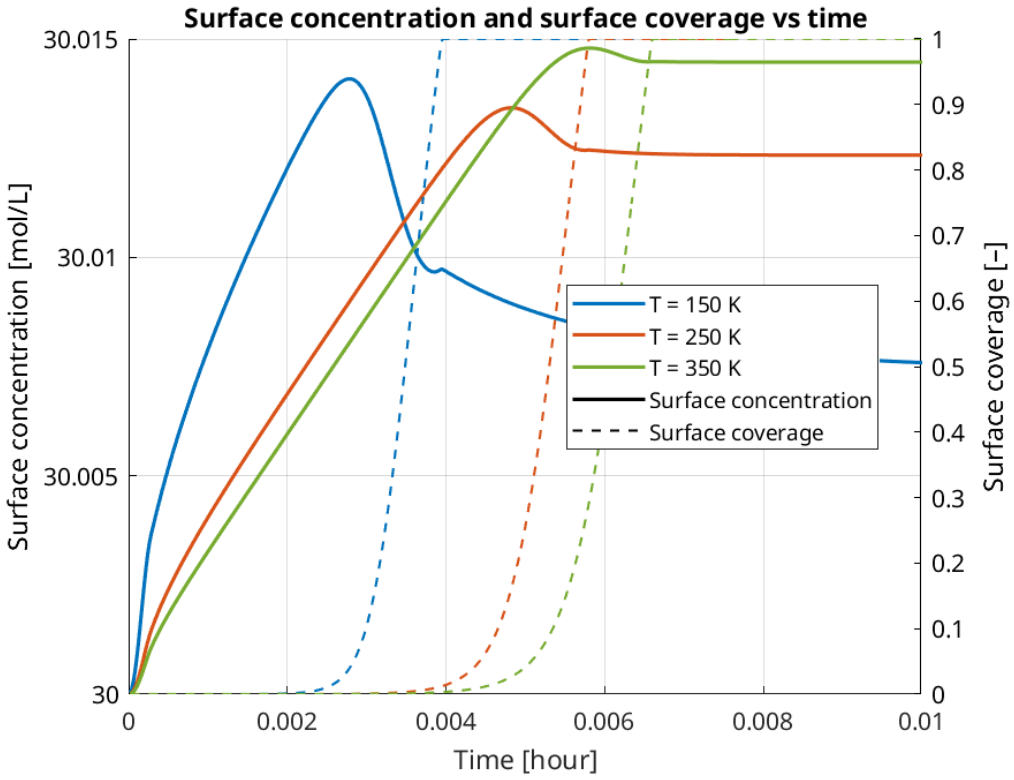

Figure 7: Surface lithium concentration (solid lines, left axis) and surface coverage by plated lithium θ (dashed lines, right axis) versus time, at different temperatures. Lower temperatures result in earlier plating onset, stronger blocking effects, and reduced overall lithiation.

6 Conclusion

In this work, we extended the *BattMo* simulation platform to incorporate the dynamics of lithium plating and stripping, based on the electrochemical model proposed by Hein, Danner, and Latz [4]. This required implementing a new interfacial reaction governed by Butler–Volmer kinetics, introducing a conservation equation for plated lithium, and modifying the existing mass and charge balance equations to include the effects of surface coverage. The model also accounts for the dynamic blocking of intercalation when the electrode surface becomes fully covered with plated lithium, as well as the reactivation of intercalation during the stripping phase.

Our implementation reproduces the key qualitative features of the Heiner et al. model. We observed plating onset when the surface concentration of lithium approached a critical threshold, stabilization of plating once the electrode surface was saturated, and a transient intercalation peak during stripping due to the local re-exposure of the graphite surface. These behaviors were confirmed through various simulation regimes and are consistent with the phenomena described in the literature.

However, several aspects remain to be developed. The kinetic parameters used so far, although inspired by Arora et al. and Heiner et al., still need proper calibration against experimental data to ensure predictive accuracy. Furthermore, the current model assumes that all plated lithium is reversible, whereas in real batteries, part of the lithium becomes electronically or chemically isolated. Incorporating this *irreversibly plated lithium* would be necessary to simulate long-term degradation and capacity loss. Finally, while the model currently operates within a simplified P2D geometry, its extension to resolved 3D microstructures would allow more realistic and spatially heterogeneous plating behaviors to be captured. A full 3D geometry is essential to accurately simulate dendrite growth, a phenomenon that cannot be captured in P2D models but is critical to battery safety, as dendrites can pierce the separator and lead to internal short circuits and thermal runaway.

In summary, this work provides the structural foundation for lithium plating modeling in *BattMo*. The main physical mechanisms are now in place, and the code is ready to support further developments aimed at designing safer and more efficient lithium-ion batteries.

A *BattMo* equations

Electrolyte mass conservation	$$\frac{\partial \epsilon c_{elyte}}{\partial t} + \nabla N_+ = \frac{a i_n}{F}$$ with $$N_+ = -D_{elyte,eff}\nabla(c_{elyte}) + \frac{i_{elyte} t_+}{z_+ \nu + F} + v^{avg} c_{elyte}$$
Electrolyte charge conservation	$$\nabla(i_{elyte}) = a i_n$$ with $$i_{elyte} = -\kappa_{eff,elyte}\nabla\phi_{elyte} - \left(\frac{\partial \mu}{\partial c_{elyte}}\right)\frac{\kappa_{eff,elyte}(1-t_+)}{F z_+}$$
Electrode charge conservation	$$\nabla(i_{elde}) = -a i_n$$ with $$i_{elde} = -\sigma_{elde,eff}\nabla\phi_{elde}$$
Electrode surface reaction	$$4\pi R^2 D\frac{\partial c}{r} = \frac{a i_n}{F}$$
Electrode mass conservation	$$\frac{\partial c_{elde}}{\partial t} + \frac{1}{r^2}\frac{\partial}{\partial r}\left(r^2\left(-D_{elde}\frac{\partial c_{elde}}{\partial r}\right)\right) = 0$$
EI equation	$$I = i_{elde} + i_{elyte}$$
EI control	Ohm laws for a real circuit, fixed par the user in our case (constant current, constant voltage ...)

B Boundary conditions

Surface Reaction rate	$i_n = i_0 \left(e^{\frac{\beta F \eta}{RT}} - e^{-\frac{(1-\beta) F \eta}{RT}} \right)$ *(Butler-Volmer equation)*
Surface reaction rate coefficient	$i_0 = F k c_{elyte}^{\beta} (c_{max} - c_{elde,surface})^{\beta} c_{elde,surface}^{1-\beta}$
Overpotential	$\eta = \phi_{elde} - \phi_{elyte} - OCP(c_{elde,surface})$

Table 3: Complementary Equations

c_{elyte}	$\nabla c = 0 \quad @z = 0 \qquad c_{elyte} = c_{elyte,init} \quad @t = 0$
ϕ_{elyte}	$\nabla \phi_{elyte} = 0 \quad @z = 0$
c_{pe}	$c_{pe} = c_{pe,init} \quad @t = 0$
c_{ne}	$c_{ne} = c_{ne,init} \quad @t = 0$
ϕ_{pe}	$\nabla \phi_{pe} = -\frac{I}{\sigma_{pe,eff}} \quad @z = L_{tot}$
ϕ_{ne}	$\nabla \phi_{ne} = -\frac{I}{\sigma_{ne,eff}} \quad @z = 0$
$c_{pe,surface}$	$c_{pe,surface} = c_{ne}(R = Rp) \quad @t = 0$
$c_{ne,surface}$	$c_{pe,surface} = c_{ne}(R = Rp) \quad @t = 0$
I	Fixed by the user : $\frac{capacity}{CRate.hour}$
E	$E = OCP_{pe} - OCP_{ne} \quad @t = 0$
T	$T = T_0 \quad @t = 0$

Table 4: Boundary conditions

C Model Parameters

Table 5 lists all the parameters used in the lithium plating model, along with their physical meaning and typical values used in the simulations.

Symbol	Description	Typical Value
k_{pl}	Plating rate constant	$4.635 \cdot 10^{-9}$ m/s (Arora) or $4.635 \cdot 10^{-6}$ m/s (fast plating)
k_{ch}	Chemical intercalation rate constant	$2.89 \cdot 10^{-9}$ m/s
k_{int}	Electrochemical intercalation rate constant	$6.656 \cdot 10^{-9}$ m/s (Arora)
α	Charge transfer coefficient for plating	0.3
$n_{\text{pl}}^{\text{limit}}$	Quantity of lithium required to cover one monolayer of a particle	$1.173 \cdot 10^{-17}$ mol, See below
$n_{\text{pl},0}$	Phenomenological parameter	$1.173 \cdot 10^{-23}$ mol
r	Radius of active material particle	$1\,\mu$m
ε	Volume fraction of active material in electrode	0.5
a_{v}	Surface area per unit volume of electrode	$3 \cdot 10^5\,\text{m}^2/\text{m}^3$

Table 5: Lithium plating model parameters and their typical values.

The monolayer surface density $n_{\text{pl}}^{\text{limit}}$ is calculated as described in Hein and Latz [4], using:

$$n_{\text{pl}}^{\text{limit}} = A_{\text{tot}} \cdot d_{\text{1ML}} \cdot \nu_{\text{Li}}^{-1} \tag{26}$$

where:

- A_{tot} is the total active surface area of the particle (e.g., $A_{\text{tot}} = 4\pi r^2$ for a sphere),
- d_{1ML} is the effective monolayer thickness, estimated by:

$$d_{\text{1ML}} = \sqrt[3]{\frac{\nu_{\text{Li}}}{N_A}}$$

- $\nu_{\text{Li}} = \dfrac{M_{\text{Li}}}{\rho_{\text{Li}}}$ is the molar volume of lithium metal,
- M_{Li} is the molar mass of lithium ($\approx 6.94\,\text{g/mol}$),
- ρ_{Li} is the density of lithium ($\approx 534\,\text{kg/m}^3$),
- N_A is Avogadro's number.

References

[1] P. Arora, M. Doyle, and R. E. White. "Mathematical Modeling of the Lithium Deposition Overcharge Reaction in Lithium-Ion Batteries Using Carbon-Based Negative Electrodes". In: *Journal of The Electrochemical Society* 146.10 (Oct. 1999), p. 3543.

[2] R. Chen et al. "A review of detecting Li plating on graphite anodes based on electrochemical methods". In: *J. Mater. Chem. A* 12 (48 2024), pp. 33427–33447.

[3] M. Doyle, T. F. Fuller, and J. Newman. "Modeling of Galvanostatic Charge and Discharge of the Lithium/Polymer/Insertion Cell". In: *Journal of The Electrochemical Society* 140.6 (June 1993), p. 1526.

[4] S. Hein, T. Danner, and A. Latz. "An Electrochemical Model of Lithium Plating and Stripping in Lithium Ion Batteries". In: *ACS Applied Energy Materials* 3.9 (July 2020), pp. 8519–8531. ISSN: 2574-0962.

[5] W. Li et al. "Physics-informed neural networks for electrode-level state estimation in lithium-ion batteries". In: *Journal of Power Sources* 506 (June 2021), p. 230034.

[6] X. Lin et al. "Lithium Plating Mechanism, Detection, and Mitigation in Lithium-Ion Batteries". In: *Progress in Energy and Combustion Science* 87 (2021), p. 100953. ISSN: 0360-1285.

[7] Y. Pan et al. "Lithium Plating Detection Based on Electrochemical Impedance and Internal Resistance Analyses". In: *Batteries* 8.11 (2022). ISSN: 2313-0105.

[8] D. Ren et al. "Investigation of Lithium Plating-Stripping Process in Li-Ion Batteries at Low Temperature Using an Electrochemical Model". In: *Journal of The Electrochemical Society* 165.10 (July 2018), A2167.

[9] S. Sahu and J. M. Foster. "A continuum model for lithium plating and dendrite formation in lithium-ion batteries: Formulation and validation against experiment". In: *Journal of Energy Storage* 60 (2023), p. 106516. ISSN: 2352-152X.

[10] A. Sarkar, P. Shrotriya, and I. C. Nlebedim. "Anodic Interfacial Evolution in Extremely Fast Charged Lithium-Ion Batteries". In: *ACS Applied Energy Materials* 5.3 (2022), pp. 3179–3188. eprint: https://doi.org/10.1021/acsaem.1c03803.

[11] U. Viswanathan, T. Garrick, and M. Fortier. "Review—Lithium Plating Detection Methods in Li-Ion Batteries". In: *Journal of the Electrochemical Society* 167 (Dec. 2020).

[12] D. Wasylowski et al. "Operando visualisation of lithium plating by ultrasound imaging of battery cells". In: *Nature Communications* 15.1 (2024). Published: 2024-11-26, p. 10237. ISSN: 2041-1723.

[13] G. Zhang et al. "Lithium plating on the anode for lithium-ion batteries during long-term low temperature cycling". In: *Journal of Power Sources* 484 (2021), p. 229312. ISSN: 0378-7753.

$$\frac{\partial n_{\mathrm{Li,plated}}}{\partial t} = J_{\mathrm{plating}} \quad \longrightarrow \quad \texttt{platedCons} = \frac{\partial n_{\mathrm{Li,plated}}}{\partial t} - J_{\mathrm{plating}}$$

$$\eta_{\mathrm{pl}} = \phi_{\mathrm{el}} - \phi_{\mathrm{elyte}} + \frac{RT}{F} \ln\left(\frac{c_{\mathrm{pl}}^4}{c_{\mathrm{pl}}^4 + c_{\mathrm{pl,0}}^4}\right)$$